Title
Functional cerebral activation detected by frequency-domain near-infrared spectroscopy

Authors
Toronov, Vladislav Y
Webb, Andrew G
Choi, Jee H
et al.

Publication Date
2002-07-16

DOI
10.1117/12.475639

Functional Cerebral Activation Detected by Frequency-Domain Near-Infrared Spectroscopy

Vladislav Toronov[*], Andrew Webb[*§], Jee Hyun Choi[‡], Martin Wolf[‡], Larisa Safonova[‡], Ursula Wolf[‡], and Enrico Gratton[‡]

[*]*Beckman Institute for Advanced Science and Technology, University of Illinois at Urbana-Champaign, 405 N.Mathews, Urbana. IL 61801*

[‡]*Laboratory for Fluorescence Dynamics, Department of Physics, University of Illinois at Urbana-Champaign, 1110 West Green Street, Urbana, Illinois 61801*

[§] *Department of Electrical and Computer Engineering, University of Illinois at Urbana-Champaign*

ABSTRACT

The aim of our study was to explore the possibility of detecting hemodynamic changes in the brain using frequency-domain near-infrared spectroscopy by exploiting the phase of the intensity modulated optical signal. To obtain optical signals with the highest possible signal-to-noise ratio, we performed simultaneous NIRS-fMRI measurements, with subsequent correlation of the time courses of both measurements. The cognitive paradigm used arithmetic calculations, with optical signals acquired with sensors placed on the forehead. In three subjects we demonstrated correlation between the hemodynamic signals obtained using NIRS and BOLD fMRI.

Keywords: near infrared, brain imaging, fMRI

1. INTRODUCTION

The method of frequency-domain near-infrared spectroscopy (NIRS) of biological tissues has a number of advantages over continuous-wave NIRS [1-3]. Using numerical simulations of light propagation in the human head Firbank et al. [4] showed that the spatial profile of the sensitivity of phase to changes in optical properties spreads deeper into the brain tissue compared to the sensitivity profile of the amplitude. Also, frequency-domain NIRS allows better separation of absorption and scattering properties of tissue [1], which is important for imaging heterogeneous tissues [5]. However, it is usually difficult to obtain a sufficiently high signal-to-noise ratio in the phase signal to perform dynamic measurements. Although many results on measuring brain hemodynamics using continuous-wave NIRS have been published [6-10], no measurement of hemodynamic changes using the phase of frequency-domain NIRS signal have been reported to date. The goal of the study presented here was to explore the possibility of detecting hemodynamic changes in the brain using frequency-domain NIRS.

To obtain phase signals at the highest possible signal-to-noise ratio, we performed a series of simultaneous NIRS-fMRI measurements, with subsequent correlation of the time courses of both measurements. The cognitive paradigm used arithmetic calculations, with optical signals acquired with sensors placed on the forehead. The arithmetic calculation paradigm was selected because it is known to cause activation in the regions of the frontal cortex situated under the areas of the head surface that are usually free from hair [6,7]. To measure cerebral hemodynamics independently from NIRS, simultaneous fMRI of the brain was employed. Following our previous study of functional hemodynamics in motor cortex by simultaneous NIRS and fMRI [10], we used correlation analysis to reveal correlation in the time course of NIRS signals with the cerebral hemodynamic changes.

In this study, we found that, not only can functional hemodynamic changes in a large volume of the brain tissue be detected using the phase of intensity modulated light, but also that the phase can be sensitive to relatively weak local spontaneous cerebral fluctuations.

2. INSTRUMENTATION AND EXPERIMENTAL SETUP

For NIRS measurements we used a two-wavelength (758 and 830 nm) frequency-domain (110 MHz modulation frequency) Oximeter (ISS, Champaign, IL), which had sixteen laser diodes (eight for each wavelength) and two photomultiplier tube detectors. At a wavelength of 758 nm light absorption by the deoxy-hemoglobin (HHb)

Saratov Fall Meeting 2001: Optical Technologies in Biophysics and Medicine III, Valery V. Tuchin, Editor, Proceedings of SPIE Vol. 4707 (2002) © 2002 SPIE · 0277-786X/02/$15.00

substantially exceeds absorption by the oxy-hemoglobin (O_2Hb), while at 830 nm the O_2Hb absorption is much higher than the HHb absorption. The laser diodes operated in a sequential multiplexing mode with 40 ms "on" time for each diode. The whole acquisition cycle for 16 light sources was 640 ms. Light emitted by the laser diodes was guided to the tissue through 10m long multi-mode silica optical fibers (CUDA, FL). Two 10m long glass fiber bundles collected the scattered light and guided it to the detectors. The paired (758 and 830 nm wavelength) source fibers were attached to the sensor where the source-detector distance varied between 2.5 and 3.6 cm. Phase changes at different source-detector channels were averaged and then used to calculate the change in deoxyhemoglobin (see Section 3).

Magnetic resonance imaging was performed using a 1.5 Tesla whole body MR scanner (Signa, General Electric Medical Systems, Milwaukee, WI) equipped with echospeed gradients and a standard circularly polarized birdcage head coil. Sagittal T_1-weighted localizer scans were used to determine the correct plane for the functional scans. Gradient-echo echo-planar images were acquired using a data matrix of 64 x 64 complex points, TR=1280 ms, TE = 40 ms, FOV = 240 mm, slice thickness = 7 mm, no inter-slice gap, receiver bandwidth 62.5 kHz, and flip angle 60°. Multi-modality radiological markers (IZI Medical Products Corp, Baltimore, MD) were embedded into the optical sensor to facilitate correct orientation of the MRI slices with respect to the sensor and to enable recovery of the sensor orientation for data analysis.

3. DATA ANALYSIS

The major absorbers of near-infrared light in the human tissues are oxy- and deoxyhemoglobin. Changes in the oxy- and deoxyhemoglobin concentrations ($\Delta[O_2Hb]$ and Δ [HHb], respectively) can be related to the changes of the tissue absorption coefficient $\Delta\mu_a^\lambda$ at the wavelength λ as

$$\Delta\mu_a^\lambda = \Delta[O_2Hb]\varepsilon_{[O_2Hb]}^\lambda + \Delta[HHb]\varepsilon_{[HHb]}^\lambda, \qquad (1)$$

where $\varepsilon_{[O_2Hb]}^\lambda$ and $\varepsilon_{[HHb]}^\lambda$ are the extinction coefficients of oxy- and deoxyhemoglobin [11]. On the other hand, $\Delta\mu_a^\lambda$ can be related to the changes in the recorded near-infrared signal using solutions of the diffusion equation describing the transport of light in the highly scattering medium. The simplest solution of the frequency-domain diffusion equation gives the following equation for the phase [12]:

$$\phi = r\left(\frac{\mu_a}{2D}\right)^{1/2}[(1+x^2)^{1/2}-1]^{1/2}, \qquad (2)$$

where r is the distance from the source to the point of measurement, μ'_s is the reduced scattering coefficient, and $D=(3\mu_a+3\mu'_s)^{-1}$ is the diffusion coefficient. The value of the dimensionless parameter $x=\omega/c\mu_a$ is small at the modulation frequency ω of our instrument (110 MHz). Eq. (2) is valid for an infinite homogeneous scattering medium and gives a good approximation to the exact solution for a homogeneous semi-infinite medium in the case of a large source-detector distance ($r \gg D$) [12]. Although the optical properties of the head are not homogeneous, Eq. (2) may be used for qualitative estimation of the time course of changes occurring in the brain provided that there are no significant fluctuations in the extracranial tissue. Given the small size of x and keeping in mind that for human tissues $\mu_a \ll \mu'_s$, one can see that the phase is proportional to $1/\sqrt{\mu_a}$. This shows that a small change in the absorption coefficient will produce a proportional decrease in the values of ϕ. Assuming that no significant change in the scattering occurs due to changes in the oxy- and deoxyhemoglobin concentrations, changes in the recorded signal can be related to small absorption changes as:

$$\Delta\varphi = -\sigma_\phi \Delta\mu_a, \qquad (3)$$

where σ_ϕ is the phase differential path length factors (DPF) [13]. Thus, the time course of small changes in the absorption at a given wavelength can be obtained from the changes in the phase up to the DPF. By measuring changes in the absorption at two wavelengths one can obtain Δ[HHb] from Eqn. (1):

$$\Delta[\mathrm{HHb}] = \frac{\Delta\mu_a^{\lambda 2}\varepsilon_{HbO2}^{\lambda 1} - \Delta\mu_a^{\lambda 1}\varepsilon_{HbO2}^{\lambda 2}}{\varepsilon_{HbO2}^{\lambda 1}\varepsilon_{Hb}^{\lambda 2} - \varepsilon_{Hb}^{\lambda 1}\varepsilon_{HbO2}^{\lambda 2}}. \quad (4)$$

It is known that the blood oxygen level dependent (BOLD) fMRI signal (the change in the intensity of the EPI images) is due to the changes in the deoxyhemoglobin concentration [10]. Namely, the increase of the BOLD signal corresponds to a decrease in [HHb]. The $-\Delta$[HHb] time series obtained from the phase records with original acquisition period of 640 ms were locked to the fMRI acquisition period (1280 ms) and then used as an indicator function (a predictor) in the correlation analysis of the fMRI data.

For the analysis of fMRI data we used the MEDx 3.4 image processing package (Sensor Systems, Inc.). Every measurement produced 500 sets of six axial 2D EPI slices (64×64 matrix). with a repetition time of 1280 ms. The time series corresponding to the EPI image intensity (the BOLD signal) at each voxel were cross-correlated with the predictor ($-\Delta$[HHb] time series) to calculate the correlation coefficient. Values of correlation coefficients were then transformed to a *z*-score [14]. Statistically significant z-values were used to obtain correlation maps [14,15].

To obtain fMRI correlation maps showing activation due to the task a smoothed boxcar predictor function instead of $-\Delta$[HHb] time series was used. The maximum of this predictor function coincided with the middle of the activation periods, and the minimum corresponded to the middle of the relaxation periods. Correlation coefficients were calculated using the autocorrelation correction and assuming a hemodynamic response delay of 5 s. Statistically significant z-values were used to obtain maps showing activated regions.

4. RESULTS

The pairs of numbers separated by the "+" symbol were presented to the subjects using the fiber-optic goggles connected to a computer outside the magnet room. Every subject performed six 40s long calculation trials separated by the 20s periods of fixation. During fixation periods only the "+" symbol was presented. The beginning of the fMRI recording was triggered by the program presenting the stimulus. The beginning of the fMRI recording and every activation period were marked in the NIRS data to provide synchronization between fMRI and optical data records.

Seven healthy right-handed 20-38 year old subjects were screened. The optical sensor was attached to the left or right side of the subject's forehead above the eyebrow and the sinuses. The source-detector line was oriented parallel to the eyebrow. After the analysis of activation measurements were repeated with those subjects who exhibited activation under the non-hairy area of the forehead with the optical sensor attached to the place where the activation occurred during the first measurement. The above protocol was approved by the Institutional Review Board (Protocol number 01075.)

Analyzing task-related brain activation from fMRI data we found that in all subjects the calculation stimulus caused most pronounced activation (in terms of *z*-score) in dorsal lateral areas of the frontal lobe, which were under the hairy skin and away from the optical sensor location. In some subjects activation was also detected in the lower part of the superior and middle frontal gyri under the non-hairy skin. However, during the second measurement the frontal activation was reproduced at exactly the same location only in two subjects. In one subject activation under the optical sensor was detected during the first measurement.

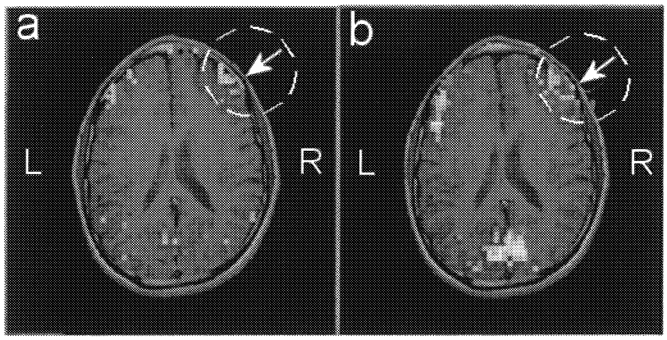

Fig.1. (a) Correlation maps obtained by temporal correlation of BOLD fMRI signal with –Δ[HHb] signal calculated using phase at 758 nm and 830 nm; (b) functional activation map produced by correlation with a stimulus-locked boxcar function. In both maps arrows point at the location of the center of the optical sensor. Letters 'L' and 'R' indicate left and right sides of the head, respectively.

Statistically significant correlation in the cortical tissue near the location of the optical sensor was detected using both intensity and phase data in all three subjects who showed activation in the area of NIRS measurement. Fig. 1 displays thresholded statistical images (z-score>4.8) showing statistically significant temporal correlation of the BOLD fMRI signal with the –Δ[HHb] signal obtained from the phase data (Fig.1 (a)) and the activated areas in the brain obtained by correlation of the fMRI signals with the smoothed boxcar predictor (Fig.1 (b)). The arrows in both subfigures point to the location of the center of the optical sensor. In both subfigures the threshold z-score value is the same and corresponds to the critical value for the activation map (Fig. 1 (b)), which had the highest critical value of the three (determined from the statistical significance analysis [14,15]). In Fig. 1 one can see that almost the same group of voxels that shows correlation with –Δ[HHb] signal obtained from the phase data also exhibits functional activation (located within the circled area near the sensor location). Apart from the circled right frontal area, where the sensor was positioned, Fig. 1(b) also shows activation in the left prefrontal area and in the occipital area in the back of the brain. Although these areas are more activated than the one located near the optical sensor, they exhibit lower correlation with phase- generated –Δ[HHb] signals than the circled areas in Figs. 1 (a). This indicates that those may be the local cerebral hemodynamic changes including non-task-related fluctuations that contribute to the changes in the optical signals. Correlation was also detected in the slices adjacent to the one shown in Fig. 1. The correlation of –Δ[HHb] signals with BOLD signals in some groups of voxels situated away from the sensor location could be due to correlation of local hemodynamic changes in different parts of the brain.

5. CONCLUSION

We demonstrated correlation in hemodynamic signals obtained from the phase of frequency-domain NIRS and BOLD fMRI data, which were simultaneously recorded during brain activation. This is the first-time demonstration of the possibility of using the phase of the intensity-modulated optical signal for the detection of hemodynamic changes in the human brain. Our results show that the DPF method correctly reproduces the time course of the cerebral hemodynamic signals.

REFERENCES

1. Gratton E., Mantulin W.W., vande Ven M.J., Fishkin J.B., Maris, M.B., and B. Chance, The possibility of a near-infrared imaging system using frequency-domain methods, Proc. Third Intl. Conf.: Peace through Mind/ Brain Science, 183-189, Hamamatsu City, Japan (1990)
2. Patterson M.S., Moulton J.,D., Wilson B.C., Frequency-domain reflectance for the determination of the scattering and absorption properties of tissue, Appl. Optics **30**, 4474-4476 (1991b)
3. Tromberg B., Svaasand L.O., Tsay T., Haskell R.C., Properties of photon density waves in multiple-scattering media, Appl. Optics **32**, 607-616 (1993)
4. Firbank M., Okada E., Delpy D.T., A theoretical study of the signal contribution of regions of the adult head to near-infrared spectroscopy studies of visual evoked responses, Neuroimage, **8**(1), 69-78 (1998)

5. McBride T.O., Pogue B.W., Osterberg U.L., Paulsen K.D., Separation of absorption and scattering heterogeneities in NIR tomographic imaging of tissue, in *Biomedical Topical Meetings,* OSA Technical Digest (Optical Society of America, Washington DC, 2000), pp.339-341.
6. Chance B., Zhuang Z., Unah C., Alter C., Lipton L., Cognition-activated low-frequency modulation of light absorption in human brain, Proc. Natl. Acad. Sci. U S A. **90**(8),3770-4 (1993)
7. Chance B, Anday E., Nioka S., Zhou S., Hong L., Worden K., Li C., Murray T.,Ovetsky Y., Pidikiti D. and Thomas R., A novel method for fast imaging of brain function, non-invasively, with light, Opt. Express **2** (10), 411-423 (1998)
8. Villringer A., Chance B., Non-invasive optical spectroscopy and imaging of human brain function, Trends Neurosci. **20**(10), 435-42 (1997)
9. Toronov V., Wolf M., Michalos A., and Gratton E.. Analysis of cerebral hemodynamic fluctuations measured simultaneously by magnetic resonance imaging and near-infrared spectroscopy. WA5, Proc. OSA Technical Digest, Biomedical Topical Meeting (2000b)
10. Toronov V., Webb A., Choi J.H., Wolf M., Michalos A., Gratton E., and Hueber D., Investigation of human brain hemodynamics by simultaneous near-infrared spectroscopy and functional magnetic resonance imaging, Med. Phys. J. 28(4), 521-527(2001)
11. Wray S., Cope M., Delpy D.T., Wyatt J.S., and Reynolds E.O., "Characterization of the near infrared absorption spectra of cytochrome aa3 and haemoglobin for the non-invasive monitoring of cerebral oxygenation", Biochim. Biophys. Acta **933**(1),184-192 (1988).
12. Fantini, S., M. A. Franceschini and E. Gratton., Semi-infinite geometry boundary problem for light migration in highly scattering media: a frequency-domain study in the diffusion approximation, J. Optical Soc. of Amer.**11**(10), 2128-2138 (1994b).
13. Fantini S., Hueber D., Franceschini M.A., Gratton E., Rosenfeld W., Stubblefield P.G., Maulik D., Stankovic M.R., Non-invasive optical monitoring of the newborn piglet brain using continuous-wave and frequency-domain spectroscopy, Phys. Med. Biol. **44**(6), 1543-1563 (1999).
14. Miller, I. and Freund, J. E. *Probability and Statistics for Engineers*, Prentice-Hall, (1977).
15. Friston, K. J., Jezzard, P. and Turner, R., Analysis of Functional MRI Time-Series. Human Brain Mapping **1**,153-171 (1994).